

UNIVERSIDAD DE CONCEPCIÓN



CENTRO DE INVESTIGACIÓN EN
INGENIERÍA MATEMÁTICA (CI²MA)



Numerical identification of parameters for strongly degenerate
parabolic equations by discrete mollification

CARLOS D. ACOSTA, RAIMUND BÜRGER,
CARLOS E. MEJIA

PREPRINT 2011-18

SERIE DE PRE-PUBLICACIONES

NUMERICAL IDENTIFICATION OF PARAMETERS FOR STRONGLY DEGENERATE PARABOLIC EQUATIONS BY DISCRETE MOLLIFICATION

CARLOS D. ACOSTA, RAIMUND BÜRGER, AND CARLOS E. MEJÍA

ABSTRACT. Numerical methods for the reliable and efficient identification of parameters defining the flux function and the diffusion coefficient of a strongly degenerate parabolic equation are of great importance in applicative areas including a sedimentation-consolidation model and a diffusively corrected kinematic traffic model. This problem can be treated by repeatedly solving the corresponding direct problem under systematic variation of an initially guessed set of model parameters, with the aim of successively minimizing a cost functional that measures the distance between a space- or time-dependent observation and the corresponding numerical solution. The direct problem is solved herein by a version of a well-known explicit, monotone three-point finite difference scheme. This version is obtained by replacing the standard conservative three-point finite difference discretization of the diffusive term by a formula that involves a discrete mollification operator. The mollified scheme occupies a larger stencil but converges under a less restrictive CFL condition, which allows to employ a larger time step than for the basic scheme. By numerical experiments it is demonstrated that despite additional computational effort, the mollified scheme leads to gains in CPU time for the parameter identification procedure. Moreover, results are also favorable compared with the basic scheme in terms of the error level and the sensitivity with respect to the initial guess and noise in the context of parameter recognition problems.

1. INTRODUCTION

1.1. **Scope.** We are interested in the numerical identification of unknown parameters appearing in the flux and diffusion terms for the following initial-boundary value problem (IBVP) for a strongly degenerate parabolic equation in one space dimension:

$$u_t + f(u)_x = A(u)_{xx}, \quad (x, t) \in \Omega_T := (0, L) \times (0, T], \quad T > 0, \quad (1.1a)$$

$$u(x, 0) = u_0(x), \quad x \in [0, L], \quad (1.1b)$$

$$f(u) - A(u)_x|_{x=0} = \psi_0(t), \quad t \in (0, T], \quad (1.1c)$$

$$f(u) - A(u)_x|_{x=L} = \psi_L(t), \quad t \in (0, T], \quad (1.1d)$$

where A is an integrated diffusion coefficient, i.e.,

$$A(u) = \int_0^u a(s) ds, \quad a(u) \geq 0. \quad (1.2)$$

The diffusion function a is assumed to be integrable and is allowed to vanish on u -intervals of positive length, on which (1.1a) turns into a first-order hyperbolic conservation law, so that (1.1a) is *strongly degenerate parabolic*. On the other hand, we assume that f is piecewise smooth and Lipschitz continuous. Under suitable choices of the functions f , a , ψ_0 and ψ_L the IBVP (1.1) may describe a variety of real processes. We here focus on (1.1) as a model of the sedimentation-consolidation process of a solid-liquid suspension [1, 2] and on a variant of this problem that describes the evolution of the local car density on a finite road segment for a diffusively corrected kinematic traffic model [3, 4].

Date: July 3, 2011.

^AUniversidad Nacional de Colombia, Department of Mathematics and Statistics, Manizales, Colombia. E-Mail: cdacostam@unal.edu.co.

^BCI²MA and Departamento de Ingeniería Matemática, Facultad de Ciencias Físicas y Matemáticas, Universidad de Concepción, Casilla 160-C, Concepción, Chile. E-Mail: rburger@ing-mat.udec.cl.

^CUniversidad Nacional de Colombia, Department of Mathematics, Medellín, Colombia. E-Mail: cemejia@unal.edu.co.

Due to its strongly degenerate parabolic nature and the nonlinearity of the convective flux, solutions of (1.1a) are, in general, discontinuous even if u_0 is smooth, and need to be defined as weak solutions along with an entropy condition to select the physically relevant solution, the *entropy solution*. For the definition, existence and uniqueness of entropy solutions of (1.1) we refer to [5]. For a short general introduction to the well-posedness analysis of strongly degenerate parabolic equations and an up-to-date list of references we refer e.g. to the introductory parts of [6].

In the present work we are interested in methods of parameter identification that are based on repeated numerical solutions of the direct problem (1.1) under successive variation of parameters appearing in the coefficient functions f and a . A numerical scheme suitable for the solution of the direct problem is the explicit, conservative monotone finite difference scheme first introduced by Evje and Karlsen in [7] for initial value problems of (1.1a), and then adapted to initial-boundary value problems [1, 8].

To describe the essential advantage in using mollified versions of this scheme, assume that Δt and Δx are the corresponding time step and meshwidth of a Cartesian grid introduced on Ω_T , and define $\lambda := \Delta t/\Delta x$ and $\mu := \Delta t/\Delta x^2 = \lambda/\Delta x$. Then the scheme from [1, 7], henceforth called *basic scheme*, converges to the unique entropy solution of (1.1) provided that the following CFL condition is satisfied:

$$\lambda \|f'\|_\infty + 2\mu \|a\|_\infty \leq 1. \quad (1.3)$$

In the basic scheme, the term $A(u)_{xx}$ is discretized conservatively by standard second finite differences of $A(u)$. The discrete mollification method provides an alternative conservative, centered discretization of $A(u)_{xx}$ on a stencil of in total $2\eta + 1$ points, where η is a parameter. It is shown in [9] that this device, which defines what we call *mollified scheme*, preserves monotonicity and convergence of the basic scheme, but that these properties hold under the CFL condition

$$\lambda \|f'\|_\infty + 2\mu\varepsilon_\eta \|a\|_\infty \leq 1, \quad (1.4)$$

where $\varepsilon_\eta < 1$. (For the values $\eta = 3$, $\eta = 5$ and $\eta = 8$ and the particular mollification weights considered herein, we get $\varepsilon_3 = 0.7130$, $\varepsilon_5 = 0.3969$ and $\varepsilon_8 = 0.1960$, respectively.) Clearly, condition (1.4) is more favorable than (1.3) since it shows that for a given value of Δx , mollified schemes may proceed by larger time steps. As was shown in [9], these schemes are even competitive in efficiency (compared with the basic scheme) in terms of error reduction per CPU time despite the fact that additional effort for the evaluation of wider stencils is involved, and slightly more numerical diffusion is introduced. For this reason, mollified schemes are an attractive option for computations that are usually time consuming, such as parameter identification problems since the same IBVP (but with varied parameters) has to be solved repeatedly. It is the purpose of the present work to demonstrate that mollified schemes are indeed competitive for parameter identification and give rise to savings in CPU time.

1.2. Related work. The discrete mollification method is a convolution-based filtering procedure suitable for the regularization of ill-posed problems and for the stabilization of explicit schemes for the solution of PDEs. With respect to numerical identification of coefficients, the mollification method has shown its advantages in different settings, for instance, diffusion coefficients, linear [10] and nonlinear [11] and right-hand side forcing terms in parabolic equations with time fractional derivatives [12].

Inverse problems for strongly degenerate parabolic equations are of particular interest in the context of the sedimentation-consolidation model. In fact, in applications such as wastewater treatment and mineral processing, the reliable extraction of material-specific parameters appearing in the model functions f and a from laboratory experiments permits to simulate the operation and control of continuous clarifier-thickeners handling the same material [13, 14]. The first approaches to solve this problem numerically were based on the numerical solution of a suitable adjoint problem [15, 16]. In particular, these papers address the theoretical issue of identifiability and partially prove the existence of solutions for the identification problem. Furthermore, they include numerical schemes and numerically solved experiments which include either noisy or simulated data. In [17], the authors introduce a numerical scheme for the simultaneous identification of several parameters and include very well designed experiments to illustrate the quality of the recovery. Likewise, reference [18] is focused on the numerical identification of unknown ingredients with the important

feature of allowing noisy data in one of the examples. In all cases it turns out that the parameters appearing in common semi-empirical formulas are associated with strongly differing sensitivities.

The present paper is focused on the numerical identification problem, and we do not address theoretical issues related to identifiability of the coefficients. As in the references cited above, the identification problem is formulated through the minimization of a suitable cost function. For the numerical solution of the direct problem, we implement two explicit schemes, the basic scheme from [1, 7] and the mollified scheme introduced in [9]. Our identification methodology is quite competitive in terms of suitability and CPU time. The numerical experiments illustrate the quality of identifications even in the presence of noisy data.

1.3. Outline of the paper. The remainder of the paper is organized as follows. In Section 2 we recall the definition and summarize some properties of the discrete mollification operator, which is the key ingredient of the mollified scheme. In Section 3 we outline the sedimentation-consolidation and traffic models (Sects. 3.1 and 3.2, respectively), and introduce the basic and mollified numerical schemes for the approximation of (1.1a) (Sect. 3.3). Section 4 describes the solution of the parameter identification problem. To this end, we formulate in Sect. 4.1 the (continuous) inverse problem as a parameter identification problem in terms of a cost functional which we seek to minimize, and which measures the distance between the observed data and calculated portions of the solution of the direct problem. Then, in Sect. 4.2, we provide a discrete formulation of this problem by replacing the exact solution of the direct problem by a numerical one, and in Sect. 4.3 the Nelder-Mead simplex method used to successively minimize the cost functional is addressed. Four numerical examples are presented in Section 5 (Sects. 5.1–5.4), three of them related to the sedimentation-consolidation model and one to the traffic model. Conclusions that can be derived from the numerical results are summarized in Sect. 5.5.

2. THE DISCRETE MOLLIFICATION OPERATOR

The discrete mollification method [19, 20] is based on replacing a discrete set of data $y = \{y_j\}_{j \in \mathbb{Z}}$, which may consist of evaluations or cell averages of a real function $y = y(x)$ at equidistant grid points $x_j = x_0 + j\Delta x$, $\Delta x > 0$, $j \in \mathbb{Z}$, by its mollified version $J_\eta y$, where J_η is the *discrete mollification operator* defined by

$$[J_\eta y]_j := \sum_{i=-\eta}^{\eta} w_i y_{j-i}, \quad j \in \mathbb{Z}.$$

Here, the support parameter $\eta \in \mathbb{N}$ indicates the width of the mollification stencil, and the weights w_i satisfy $w_i = w_{-i}$ and $0 \leq w_i \leq w_{i-1}$ for $i = 1, \dots, \eta$ along with $w_{-\eta} + \dots + w_{\eta-1} + w_\eta = 1$. The weights w_i are obtained by numerical integration of the truncated Gaussian kernel $\kappa_{p\delta}$ with parameters $\delta > 0$ and $p > 0$:

$$\kappa_{p\delta}(t) := \begin{cases} A_p \delta^{-1} \exp(-t^2/\delta^2) & \text{for } |t| \leq p\delta, \\ 0 & \text{otherwise,} \end{cases} \quad \text{where } A_p := \left(\int_{-p}^p \exp(-s^2) ds \right)^{-1}.$$

This kernel satisfies $\kappa_{p\delta} \geq 0$, $\kappa_{p\delta} \in C^\infty(-p\delta, p\delta)$, $\kappa_{p\delta} = 0$ outside $[-p\delta, p\delta]$, and $\int_{\mathbb{R}} \kappa_{p\delta} = 1$. Then we compute the weights by

$$w_i := \int_{(i-1/2)\Delta x}^{(i+1/2)\Delta x} \kappa_{p\delta}(-s) ds, \quad i = -\eta, \dots, \eta. \quad (2.1)$$

Usually $p = 3$ is taken and δ , whose role is to determine the shape of the Gaussian bell of the kernel, is considered as regularization parameter, and it is estimated by methods like Generalized Cross Validation (GCV) [20, 21]. In any case, in this work, as was done in previous papers [9, 22, 23, 30, 31], the main relationship between δ and η is given by $\delta = (\eta + 1/2)\Delta x/p$. This choice generates weights $w_{-\eta}, \dots, w_\eta$ that are independent of Δx . The resulting values of w_i for several values of η and $p = 3$ are given in Table 1.

We conclude this section with some approximation and stability results. In what follows, we denote by Δ_+ , Δ_- and Δ_0 the spatial forward, backward, and centered difference operators defined by $\Delta_+ z_j := z_{j+1} - z_j$, $\Delta_- z_j := z_j - z_{j-1}$, and $\Delta_0 z_j := (z_{j+1} - z_{j-1})/2$, respectively.

η	$i = 0$	$i = 1$	$i = 2$	$i = 3$	$i = 4$	$i = 5$	$i = 6$	$i = 7$	$i = 8$
0	1								
1	0.84272	0.07864							
2	0.60387	0.19262	5.4438e-3						
3	0.45556	0.23772	3.3291e-2	1.2099e-3					
4	0.36266	0.24003	6.9440e-2	8.7275e-3	4.7268e-4				
5	0.30028	0.22625	9.6723e-2	2.3430e-2	3.2095e-3	2.4798e-4			
6	0.25585	0.20831	0.11241	4.0192e-2	9.5154e-3	1.4905e-3	1.5434e-4		
7	0.22270	0.19058	0.11942	5.4793e-2	1.8403e-2	4.5234e-3	8.1342e-4	1.0697e-4	
8	0.19708	0.17444	0.12097	6.5725e-2	2.7973e-2	9.3255e-3	2.4348e-3	4.9782e-4	7.9691e-5

TABLE 1. Discrete mollification weights $w_i = w_{-i}$, $i = 0, \dots, \eta$, given by (2.1) with $p = 3$.

Lemma 1. *The discrete mollification operator is conservative. Specifically, it can be written in the form $[J_\eta y]_j = y_j + (\psi_j - \psi_{j-1})$, where we define*

$$\rho_k := \sum_{i=k}^{\eta} w_i, \quad k = -\eta, \dots, \eta; \quad \psi_j := \sum_{k=1}^{\eta} \rho_k (y_{j+k} - y_{j-k+1}).$$

Assume that g is a sufficiently smooth real function, and set $y_j = g(x_j)$. Then, by using Taylor expansions of y_{j+i} with respect to y_j one can show that

$$[J_\eta y]_j = \sum_{i=-\eta}^{\eta} w_{-i} y_{j+i} = y_j + \frac{\Delta x^2}{2C_\eta} g''(x_j) + \frac{\Delta x^4}{24} \sum_{i=-\eta}^{\eta} i^4 w_{-i} g^{(4)}(\xi_{j,i}) \quad (2.2)$$

(see [23] for details), where $\xi_{j,i}$ is a real number between x_j and x_{j+i} and we define

$$C_\eta := \left(\sum_{i=-\eta}^{\eta} i^2 w_{-i} \right)^{-1}.$$

Theorem 1. *Let $g \in C^4(\mathbb{R})$ with $g^{(4)}$ bounded on \mathbb{R} , and set $y_j := g(x_j)$. Assume that the data $\{y_j^\varepsilon\}_{j \in \mathbb{Z}}$ satisfy $|y_j^\varepsilon - y_j| \leq \varepsilon$ for all $j \in \mathbb{Z}$. Then $|[J_\eta y^\varepsilon]_j - [J_\eta y]_j| \leq \varepsilon$ for all $j \in \mathbb{Z}$. Additionally, for each compact set $K = [a, b]$ there exists a constant $C = C(K)$ such that*

$$\left| [J_\eta y]_j - g(x_j) - \frac{\Delta x^2}{2C_\eta} g''(x_j) \right| \leq C \Delta x^4 \quad \text{for all } j \in \mathbb{Z}. \quad (2.3)$$

Moreover, the following inequalities hold for all $j \in \mathbb{Z}$, where C is a different constant in each inequality:

$$\begin{aligned} |[J_\eta y]_j - g(x_j)| &\leq C \Delta x^2, & |\Delta_0 [J_\eta y]_j - \Delta x g'(x_j)| &\leq C \Delta x^3, \\ |\Delta_+ [J_\eta y]_j - \Delta x g'(x_j)| &\leq C \Delta x^2, & |\Delta_- \Delta_+ [J_\eta y]_j - \Delta x^2 g''(x_j)| &\leq C \Delta x^4. \end{aligned} \quad (2.4)$$

Details of the proofs of Lemma 1 and of (2.4) can be found in [23], while (2.3) is a way of rewriting (2.2).

3. APPLICATIVE MODELS AND DISCRETIZATION OF THE DIRECT PROBLEM

3.1. Sedimentation-consolidation model. According to a well-known sedimentation-consolidation model (see, e.g., [2, 13, 24] and references cited in these works), (1.1) can be understood as a model for the settling of a flocculated suspension of small solid particles dispersed in a viscous fluid, where the solution of (1.1), $u = u(x, t)$, is the local solids concentration as a function of x and t . For batch settling in a closed column of height L we set $\psi_0 \equiv 0$ and $\psi_L \equiv 0$, and u_0 denotes the initial concentration. The material specific function f describes the effect of hindered settling. We employ here the following typical parametric expression:

$$f(u) = \begin{cases} v_\infty u (1 - u/u_{\max})^C & \text{for } 0 < u < u_{\max}, \\ 0 & \text{otherwise,} \end{cases} \quad \text{with parameters } v_\infty < 0 \text{ and } C > 1, \quad (3.1)$$

where v_∞ is the settling velocity of a single particle in an unbounded fluid and $0 < u_{\max} \leq 1$ is a (nominal) maximal solids concentration. The function A is given by (1.2), where we define

$$a(u) = -\frac{f(u)\sigma'_e(u)}{(\varrho_s - \varrho_f)gu}, \quad (3.2)$$

where ϱ_s and ϱ_f are the solid and fluid density, respectively, g is the acceleration of gravity, and $\sigma'_e(u) = d\sigma_e/du$ is the derivative of the material-specific effective solid stress function $\sigma_e = \sigma_e(u)$, which is usually assumed to satisfy $\sigma'_e(u) = 0$ for $u \leq u_c$ and $\sigma'_e(u) > 0$ for $u > u_c$, where $0 \leq u_c \leq u_{\max}$ is a critical concentration at which the solid particles start to touch each other. Clearly, $A(u) = 0$ for $0 \leq u \leq u_c$, so (1.1a) degenerates to first-order hyperbolic type on $[0, u_c]$.

Among several proposed semi-empirical approaches for σ_e we focus here on the power-law-type function

$$\sigma_e(u) = \begin{cases} 0 & \text{for } 0 \leq u \leq u_c, \\ \sigma_0[(u/u_c)^\beta - 1] & \text{for } u > u_c \end{cases} \quad (3.3)$$

with material-dependent parameters $\sigma_0 > 0$ and $\beta > 1$. The values of β , σ_0 and u_c characterize the compressibility of the sediment formed by a given material.

Values of the primitive $A(u)$ usually have to be determined by numerical quadrature. However, if f and a are given by (3.1)–(3.3) and β is an integer, then $A(u)$ can be evaluated in closed form by $A(u) = 0$ for $0 \leq u \leq u_c$ and $A(u) = \mathcal{A}(u) - \mathcal{A}(u_c)$ for $u > u_c$, where the function \mathcal{A} is defined by

$$\mathcal{A}(u) := \frac{v_\infty \sigma_0}{\Delta_\varrho g u_c^\beta u_{\max}^C} \sum_{k=1}^{\beta} \left(\prod_{l=1}^k \frac{\beta + 1 - l}{C + l} \right) (u_{\max} - u)^{C+k} u^{\beta-k}.$$

3.2. Traffic model. The strongly degenerate parabolic PDE (1.1a) also arises as a model of traffic flow on the segment $[0, L]$ of a one-directional, single-lane highway. This model is a diffusively corrected version of the well-known Lighthill-Whitham-Richards kinematic traffic model, see [3, 4]. Within that model, $u = u(x, t)$ denotes the local density of cars (measured e.g. in cars per mile), and the function f is given by one of the many semi-empirical approaches that relate traffic velocity $V = V(u)$ to the local density u via $f(u) = uV(u)$. We employ the Dick-Greenberg expression [25, 26]

$$V(u) = v_{\max} \cdot \min\{1, C \ln(u_{\max}/u)\} = v_{\max} \cdot \begin{cases} 1 & \text{for } 0 \leq u \leq u_* := u_{\max} \exp(-1/C), \\ C \ln(u_{\max}/u) & \text{for } u_* < u \leq u_{\max}, \end{cases} \quad (3.4)$$

where $C > 0$ is a parameter, u_{\max} is a maximal density and v_{\max} is the preferential (maximal) velocity a vehicle would attain on a free highway, which yields

$$f(u) = \begin{cases} u & \text{for } 0 \leq u \leq u_*, \\ Cu \ln(u_{\max}/u) & \text{for } u_* < u \leq u_{\max}, \\ 0 & \text{otherwise.} \end{cases} \quad (3.5)$$

Assume now that τ is a reaction time and L_{react} is a reaction length, where the latter may depend on $V(u)$. To be definite, we employ here, as in [3], the following formula due to Nelson [27]:

$$L_{\text{react}}(u) = \max \left\{ \frac{(V(u))^2}{2\alpha}, L_{\min} \right\}, \quad (3.6)$$

where L_{\min} is a minimal anticipation distance and α denotes a deceleration, so that the first argument in (3.6) denotes the distance required to decelerate from speed $V(u)$ to full stop at deceleration α . One may then argue that the velocity of a vehicle position x at time t does not depend on the density seen at the same point (x, t) , as in the LWR model, but rather on the density at position $x + L_{\text{react}} - V\tau$ at time $t - \tau$. An appropriate expansion of u evaluated at this displaced argument around (x, t) (see [3, 27, 28] for details) leads to the conclusion that to within an $\mathcal{O}(\tau^2 + L_{\text{react}}^2)$ error in consistency, $u = u(x, t)$ is given by (1.1a) (instead of the first-order conservation law $u_t + f(u)_x = 0$ of the LWR model) with A given by (1.2), where

$$a(u) = -uV'(u)(L_{\text{react}}(u) + \tau uV'(u)). \quad (3.7)$$

Since the function V given by (3.4) satisfies $V'(u) = 0$ for $0 \leq u \leq u_*$, the function a given by (3.7) in combination with (3.4) satisfies $a(u) = 0$ for $u < u_c := u_*$ and $u = u_{\max}$, and therefore (1.1a) is indeed strongly degenerate parabolic. Other functions V still give rise to a strongly degenerate parabolic equation if we assume that reaction time and reaction length are effective only whenever the local traffic density u exceeds a critical value u_c . This explanation is advanced in [4].

If the expressions (3.4) and (3.6) are employed, then the function A obtained via (1.2) can be expressed in closed form [3]. We here obtain $A(u) = 0$ for $0 \leq u \leq u_c$ and $A(u) = v_{\max}(\mathcal{R}(u) - \mathcal{R}(u_c))$ for $u_c < u \leq u_{\max}$, where the function \mathcal{R} is defined as follows. Fix a bound of integration $\tilde{u}_0 \in (0, u_c)$, and let $L_0 = v_{\max}^2 C^2 / (2\alpha)$ and $u^* = u_{\max} \exp(-(L_{\min}/L_0)^{1/2})$. If $u^* > u_c$, then

$$\mathcal{R}(u) = \begin{cases} \mathcal{K}(u) & \text{for } u_c \leq u \leq u^*, \\ \mathcal{K}(u^*) + (CL_{\min} - C^2\tau v_{\max})(u - u^*) & \text{for } u > u^*, \end{cases}$$

where we define the function

$$\mathcal{K}(u) = CL_0 \left\{ [(\ln u_{\max})^2 + 2 \ln u_{\max} + 2]s - 2(\ln u_{\max} + 1)s \ln s + s(\ln s)^2 \right\} \Big|_{s=\tilde{u}_0}^{s=u} - C^2\tau v_{\max}(u - \tilde{u}_0).$$

3.3. Discretization of the direct problem. The domain Ω_T is discretized by a standard Cartesian grid by setting $x_j := j\Delta x$, $j = 0, \dots, \mathcal{N}$, where $\mathcal{N}\Delta x = L$, and $t_n := n\Delta t$, $n = 0, \dots, \mathcal{M}$, where $\mathcal{M}\Delta t = T$. We assume that Δx and Δt satisfy the respective CFL conditions (1.3) and (1.4) of the methods to be introduced. We denote by u_j^n an approximate value of the cell average of $u = u(x, t)$ over the cell $[x_j, x_{j+1}]$ at time $t = t_n$, and correspondingly set

$$u_j^0 = \frac{1}{\Delta x} \int_{x_j}^{x_{j+1}} u_0(x) dx, \quad j = 0, \dots, \mathcal{N} - 1.$$

For the numerical solution of (1.1) we consider two convergent finite difference methods, namely the basic scheme [1, 7] and alternatively, its mollified version introduced in [9]. The first one has the following form, where we recall that $\lambda = \Delta t / \Delta x$ and $\mu = \Delta t / \Delta x^2$:

$$u_j^{n+1} = u_j^n - \lambda \Delta_+ F^{\text{EO}}(u_{j-1}^n, u_j^n) + \mu (A(u_{j+1}^n) - 2A(u_j^n) + A(u_j^n)). \quad (3.8)$$

The scheme (3.8) is monotone and convergent under the CFL condition (1.3). Here F^{EO} stands for the well-known Engquist-Osher flux [29].

The mollified scheme is also monotone and convergent and takes the form

$$u_j^{n+1} = u_j^n - \lambda \Delta_+ F^{\text{EO}}(u_{j-1}^n, u_j^n) + 2\mu C_\eta ([J_\eta A(u^n)]_j - A(u_j^n)). \quad (3.9)$$

This is an explicit method, however, it is enhanced with the convenient CFL condition (1.4), where $\varepsilon_\eta := C_\eta(1 - w_0)$. The values of ε_3 , ε_5 and ε_8 mentioned in Section 1.1 correspond to the parameter $p = 3$. For this value, ε_η is a decreasing function of η ; for instance, we also have $\varepsilon_{12} = 0.0988$ and $\varepsilon_{20} = 0.0392$.

The basic scheme is taken as a reference scheme, for comparison purposes. The computations at the boundaries, i.e., the implementation of the boundary conditions, will be explained in Section 5 for each of the numerical examples.

4. PARAMETER IDENTIFICATION

4.1. Inverse Problem. The inverse problem can be formulated as follows: given observation data $u^{\text{obs}}(x)$ at a time $T > 0$ and the functions u_0 , ψ_1 and ψ_2 , find the flux f and the diffusion function a of the form (3.1)–(3.3) such that the entropy solution $u(x, T)$ at time T of the problem (1.1) is as close as possible to $u^{\text{obs}}(x)$ in some suitable norm. Thus, the inverse problem consists in minimizing a cost function J which measures the distance between $u(\cdot, T)$ and u^{obs} . The inverse problem can then be formulated as follows:

$$\text{minimize } J(u(\cdot, T)) \text{ with respect to the functions } f \text{ and } a, \quad (4.1)$$

where u is the entropy solution to (1.1) corresponding to a particular choice of the flux f and the diffusion function a . A common choice for the cost function J is

$$J(u(\cdot, T)) = \frac{1}{2} \int_0^L |u(x, T) - u^{\text{obs}}(x)|^2 dx. \quad (4.2)$$

In both the sedimentation and traffic models the functions f and a are given in semi-empirical parametric forms via (3.1), (3.3) and (3.5)–(3.7), respectively, so that the inverse problem is reduced to that of finding a vector \mathbf{p} of a finite number of parameters such that the solution u of (1.1) calculated for the corresponding functions f and a minimizes $J(u(\cdot, T))$. In other words, the inverse problem is replaced by the parameter identification problem “minimize $J(u(\cdot, T))$ with respect to the parameter vector \mathbf{p} ”, where \mathbf{p} is the vector of unknown parameters and u is the entropy solution of (1.1) found with the functions f and a associated to the current values of \mathbf{p} . In what follows, we will write $J(\mathbf{p})$ instead of $J(u(\cdot, T))$, so that the parameter identification problem reads

$$\text{minimize } J(\mathbf{p}) \text{ with respect to the parameter vector } \mathbf{p}. \quad (4.3)$$

4.2. Discretization of the parameter identification problem. We define the piecewise constant function u^Δ on Ω_T by

$$u^\Delta(x, t) = u_j^n \quad \text{for } x \in [x_j, x_{j+1}), t \in [t_n, t_{n+1}), j = 0, \dots, \mathcal{N} - 1, t = 0, \dots, \mathcal{M} - 1,$$

and replace u^{obs} by a piecewise constant function $u^{\text{obs}, \Delta}$ formed by cell averages of u^{obs} as follows:

$$u^{\text{obs}, \Delta}(x) = u_j^{\text{obs}} := \frac{1}{\Delta x} \int_{x_j}^{x_{j+1}} u^{\text{obs}}(x) dx \quad \text{for } x \in [x_j, x_{j+1}), j = 0, \dots, \mathcal{N} - 1.$$

We define the following discrete analogue of the cost function defined in (4.2):

$$J^\Delta(\mathbf{p}) := \frac{1}{2} \int_0^L |u^\Delta(x, T) - u^{\text{obs}, \Delta}(x)| dx = \frac{\Delta x}{2} \sum_{j=0}^{\mathcal{N}-1} |u_j^\Delta - u_j^{\text{obs}}|^2. \quad (4.4)$$

The discrete version of the parameter identification problem (4.3) can now be formulated as follows:

$$\text{minimize } J^\Delta(\mathbf{p}) \text{ with respect to the parameter vector } \mathbf{p},$$

where the discrete cost function $J^\Delta(\mathbf{p})$ is defined by (4.4) and the numerical solution u^Δ is calculated by using the functions f and a obtained from the current values of the parameter vector \mathbf{p} . Note that each evaluation of $J^\Delta(\mathbf{p})$ (for one value of \mathbf{p}) requires the numerical solution of the direct problem (1.1).

Similarly, if instead of $u^{\text{obs}}(x)$ given at time $T > 0$, we have a time-dependent observation $u_{\text{obs}} = u_{\text{obs}}(t)$ at a fixed position $x = x_M$, then we replace u_{obs} by cell averages of the form

$$u_{\text{obs}}^\Delta(t) = u_{\text{obs}}^n := \frac{1}{\Delta x} \int_{t_n}^{t_{n+1}} u_{\text{obs}}(t) dt \quad \text{for } t \in [t_n, t_{n+1}).$$

In this way we can define an alternative cost function of the form

$$J^\Delta(\mathbf{p}) := \frac{1}{2} \int_0^T |u^\Delta(x_M, t) - u_{\text{obs}}^\Delta(t)|^2 dt = \frac{\Delta t}{2} \sum_{n=0}^{\mathcal{M}-1} |u_M^n - u_{\text{obs}}^n|. \quad (4.5)$$

4.3. Nelder-Mead simplex method. The optimization process of (4.4) and (4.5) is carried out by a restarted version of the Nelder-Mead simplex method (`fminsearch` in MATLAB). This is a derivative-free optimization method that is widely used by researchers in different fields, is very well documented but with convergence limitations [32]. Due to the lack of convergence in some cases, many modifications have been proposed. For instance, Kelley [33], Luersen et al. [34] and Zhao et al. [35] consider different ways of updating the current simplex and different restarting procedures for obtaining a descendent and deterministic method.

Our restarted strategy ends when no substantial variation of the values of the parameters is achieved. It takes the following form, where we assume that $\mathbf{p}_j = (p_j^1, \dots, p_j^K)$, i.e., we assume that K different parameters are sought:

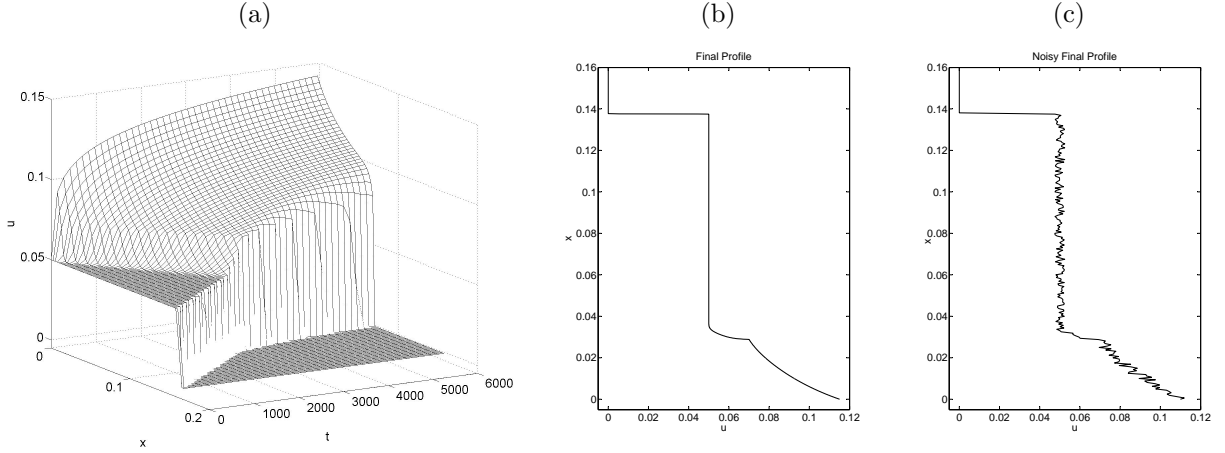


FIGURE 1. Examples 1–3: (a) reference solution, (b) profile used as u^{obs} in Examples 1 and 2 (numerical solution at transient time $T = 800$ s), (c) sample of noisy final profile for Example 3 with $\varepsilon = 0.05$.

- (1) Input \mathbf{p}_0, ϵ
- (2) for $j = 1$ to M
 - (a) $\mathbf{p}_j = \text{fminsearch}(J^\Delta, \mathbf{p}_{j-1})$
 - (b) if $\max_{1 \leq k \leq K} |(p_j^k - p_{j-1}^k)/p_{j-1}^k| \leq \epsilon$ then break, end
- (3) end

Finally, we note that only an initial value \mathbf{p}_0 for the parameter vector \mathbf{p} is needed as input, from which the `fminsearch` routine builds the initial simplex following a criterion developed by L. Pfeffer, see [36].

5. NUMERICAL EXAMPLES

For each method, the basic scheme (3.8) and its mollified version (3.9), the functionals (4.4) and (4.5) can be computed. So, we compare the performance of the restarted optimization procedure for each method. The reference solution is generated by the corresponding numerical scheme (3.8) or (3.9) on a very fine grid. In the case of the temporal observation, we choose a suitable CFL for working on a whole set of parameter values. So, the solutions can be computed with the same discretization parameters $(\Delta x, \Delta t)$. In all examples, we effectively solve a parameter *recognition* problem, which means that the observation u^{obs} or u_{obs} is generated “synthetically” not from real-world experimental data, but by a numerical solution with known parameters, possibly perturbed by the addition of some “noise”.

5.1. Example 1: sedimentation model, effect of the mollification parameter. Examples 1, 2 and 3 deal with the sedimentation model. We consider batch settling in a column of height $L = 0.16$ m and the parameter values $u_{\text{max}} = 0.5$, $g = 9.81 \text{ m/s}^2$, $\varrho_s - \varrho_f = 1660 \text{ kg/m}^3$, $v_\infty = -2.7 \times 10^{-4} \text{ m/s}$, $C = 21.5$, $\beta = 5$, $u_c = 0.07$ and $\sigma_0 = 1.2 \text{ Pa}$. The objective will be to obtain an accurate identification of the parameters u_c , σ_0 and C in eight different instances described in Table 2. Our experiments include clean and noisy observation data. Data at the instant $T = 800$ s will play the role of u^{obs} . Figures 1 (a) and (b) show the reference solution on the whole computational domain and the profile at $T = 800$ s, respectively. The restarting parameter and the tolerance parameter for the optimization are $M = 10$ and $\epsilon = 10^{-4}$ respectively.

In this case, the boundary flux functions ψ_0 and ψ_L are both zero. So, following [1, Sect. 3.2], we discretize the boundary condition at $x = 0$ as follows. We replace the expression $F^{\text{EO}}(u_{-1}^n, u_0^n) - (A_0^n - A_{-1}^n)/\Delta x$ by zero, so that from the marching formula for the basic scheme, (3.8), we obtain the following “boundary

initial guess	parameter values	initial guess	parameter values
A	$(0.7u_c, 0.7\sigma_0, 0.7C)$	E	$(1.3u_c, 0.7\sigma_0, 0.7C)$
B	$(0.7u_c, 0.7\sigma_0, 1.3C)$	F	$(1.3u_c, 0.7\sigma_0, 1.3C)$
C	$(0.7u_c, 1.3\sigma_0, 0.7C)$	G	$(1.3u_c, 1.3\sigma_0, 0.7C)$
D	$(0.7u_c, 1.3\sigma_0, 1.3C)$	H	$(1.3u_c, 1.3\sigma_0, 1.3C)$

TABLE 2. Example 1: initial guesses used for identification experiments.

IG	j	\mathbf{p}_j	E_J	e_∞	CPU [s]	j	\mathbf{p}_j	E_J	e_∞	CPU [s]
Basic scheme (3.8)						Mollified scheme (3.9) with $\eta = 3$				
A	2	(0.0697, 1.1219, 21.4706)	290	0.0651	79.863	2	(0.0695, 1.1104, 21.5067)	356	0.0746	89.43
B	4	(0.0696, 1.1111, 21.4700)	517	0.0741	90.310	4	(0.0695, 1.1105, 21.5067)	490	0.0746	89.77
C	5	(0.0697, 1.1324, 21.4700)	616	0.0564	163.74	2	(0.0695, 1.1104, 21.5067)	296	0.0747	103.1
D	3	(0.0696, 1.1252, 21.4699)	669	0.0623	127.96	5	(0.0695, 1.1103, 21.5067)	797	0.0747	155.8
E	3	(0.0696, 1.1179, 21.4700)	367	0.0684	59.662	3	(0.0696, 1.1259, 21.5075)	332	0.0617	58.19
F	6	(0.0696, 1.1117, 21.4700)	674	0.0736	108.77	3	(0.0696, 1.1294, 21.5066)	358	0.0588	61.25
G	3	(0.0696, 1.1114, 21.4700)	421	0.0738	71.391	3	(0.0695, 1.1104, 21.5068)	402	0.0747	73.08
H	2	(0.0696, 1.1180, 21.4700)	391	0.0684	64.747	5	(0.0695, 1.1104, 21.5065)	676	0.0747	119.7
Mollified scheme (3.9) with $\eta = 5$						Mollified scheme (3.9) with $\eta = 8$				
A	5	(0.0500, 0.1486, 21.5456)	685	0.8762	152.8	2	(0.0696, 1.1174, 21.5777)	293	0.0688	49.008
B	5	(0.0697, 1.1651, 21.5465)	664	0.0291	105.8	3	(0.0697, 1.1530, 21.5776)	461	0.0391	64.792
C	3	(0.0695, 1.1124, 21.5466)	486	0.0730	103.6	4	(0.0697, 1.1531, 21.5776)	649	0.0391	107.35
D	3	(0.0696, 1.1301, 21.5465)	639	0.0582	107.1	2	(0.0697, 1.1530, 21.5777)	418	0.0391	60.759
E	3	(0.0696, 1.1301, 21.5466)	445	0.0583	69.26	3	(0.0697, 1.1531, 21.5776)	535	0.0391	74.026
F	6	(0.0695, 1.0945, 21.5466)	697	0.0879	107.7	3	(0.0696, 1.1174, 21.5777)	543	0.0688	73.858
G	3	(0.0696, 1.1299, 21.5466)	485	0.0584	78.23	4	(0.0697, 1.1531, 21.5776)	576	0.0391	80.604
H	4	(0.0696, 1.1472, 21.5465)	807	0.0440	128.4	2	(0.0697, 1.1531, 21.5776)	640	0.0391	89.225

TABLE 3. Example 1: results for the basic scheme (3.8) and the mollified scheme (3.9) with $\eta = 3, 5$ and 8.

scheme” for u_0^n , which is utilized for $j = 0$ instead of (3.8):

$$u_0^{n+1} = u_0^n - \lambda F^{\text{EO}}(u_0^n, u_1^n) + \mu(A(u_1^n) - A(u_0^n)).$$

A similar formula holds at $x = L$. To compute the discrete mollification of $A(u)$, for instance at $x = 0$, we take advantage of the knowledge of $A(u_0^n)$ and its slope $\partial A(u)/\partial x|_{x=0} = f(u(0, t))$ to build a linear extrapolation of $A(u)$ at $x = 0$ beyond the boundary $x = 0$ of Ω_T . With this extension we compute $[J_\eta A(u^n)]_0$. We proceed for $[J_\eta A(u^n)]_{\mathcal{N}}$ in a similar way.

In Example 1 we employ the cost function (4.4), working with clean observation data (no noise added) and $\Delta x = L/256$. The results are summarized in Table 3. Here, j denotes the number of calls of the `fminsearch` algorithm, \mathbf{p}_j is the found vector of parameter values, E_J is the required number of computed solutions of the direct problem, e_∞ is the maximum relative error in the result for each parameter (usually due to σ_0), and CPU denotes the total CPU time of each run.

5.2. Example 2: sedimentation model, sensitivity to the choice of the initial guess. In this example we check the sensitivity of the procedure to the choice of the initial guess. For this purpose we randomly generate 100 initial guesses and carry out the identification task. Each initial guess $\mathbf{p}_0 = (u_c^0, \sigma_0^0, C^0)^T$ is generated in the form $u_c^0 = (1 + 0.3\xi_1)u_c$, $\sigma_0^0 = (1 + 0.3\xi_2)\sigma_0$ and $C^0 = (1 + 0.3\xi_3)C$, where $\boldsymbol{\xi} = (\xi_1, \xi_2, \xi_3)^T \in \mathbb{R}^3$ is a uniformly distributed random vectorial variable whose components are between -1 and 1 . The results are indicated in Table 4. Here, the average \bar{e}_∞ of e_∞ , its standard deviation σ and its confidence interval \mathcal{I}_∞ ,

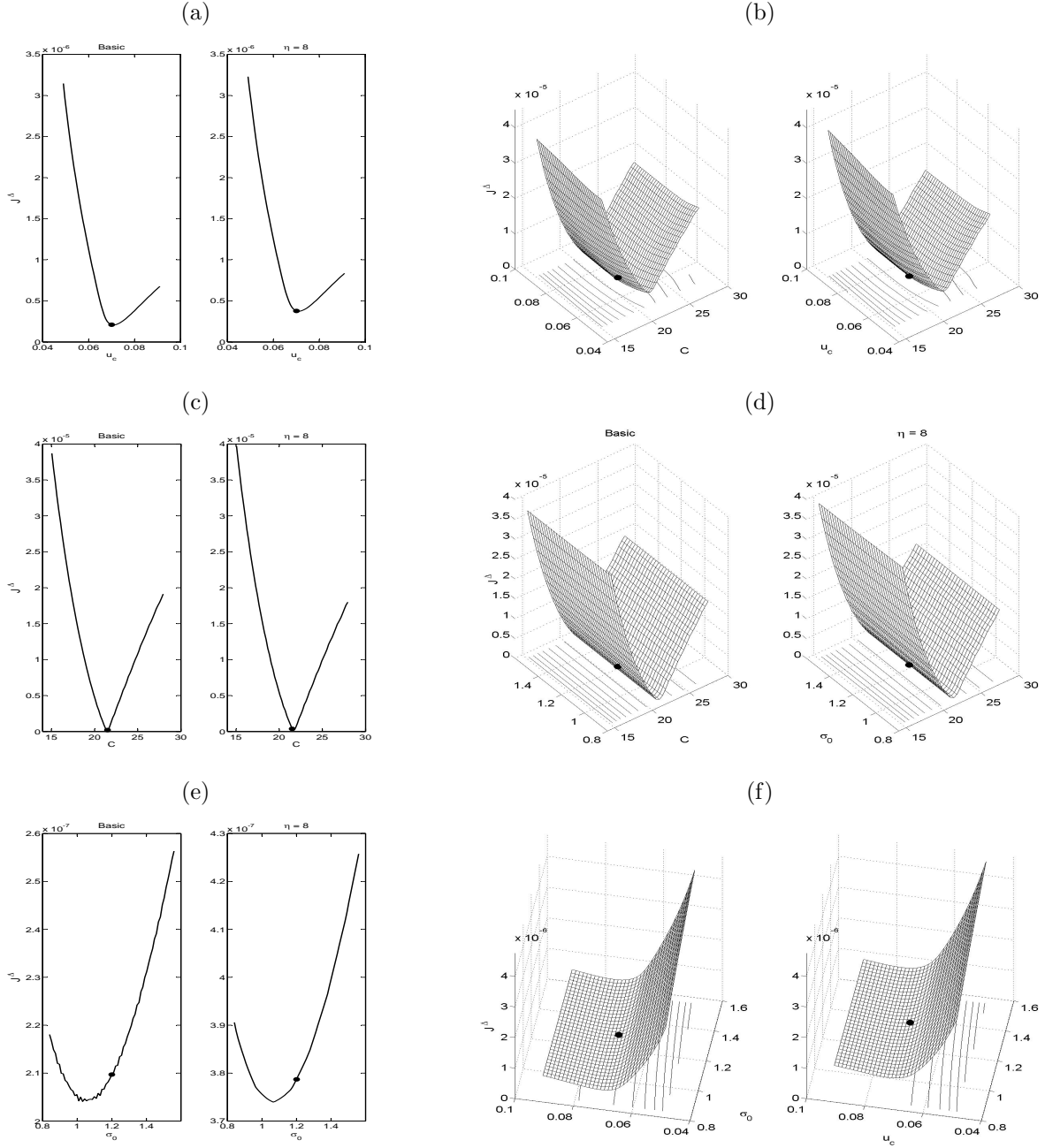


FIGURE 2. Example 2: one and two-parameter cost functional for each parameter set: (a) u_c , (b) (C, u_c) , (c) C , (d) (C, σ_0) , (e) σ_0 , (f) (u_c, σ_0) .

with a probability of 95% computed with a t -Student distribution of 99 freedom degrees, are included. Additionally, the column “# restarts” stands for the number of calls of `fminsearch` and E_J for the number of solutions of the direct problem. The corresponding total time for the 100 identifications is also indicated. The behaviour of the restarting during this test is illustrated in Figure 3. The need of less restarts when working with the mollified scheme could indicate less presence of local minima in that case.

$\Delta x/L$	Scheme	η	# restarts	E_J	$\bar{e}_\infty \pm \sigma$	\mathcal{I}_∞	CPU [min]
1/128	basic (3.8)	—	387	53693	0.1400 ± 0.0329	[0.1345, 0.1455]	49.17
	mollified (3.9)	3	340	49274	0.1295 ± 0.0338	[0.1239, 0.1351]	53.92
	mollified (3.9)	5	333	50659	0.0909 ± 0.0315	[0.0856, 0.0961]	50.91
	mollified (3.9)	8	276	41263	$0.0534 \pm 3.7182e-05$	[0.0534, 0.0534]	39.36
1/256	basic (3.8)	—	388	48842	0.0696 ± 0.0096	[0.0680, 0.0712]	136.03
	mollified (3.9)	3	398	53513	0.0739 ± 0.0081	[0.0725, 0.0752]	160.74
	mollified (3.9)	5	355	48280	0.0587 ± 0.0174	[0.0558, 0.0616]	125.46
	mollified (3.9)	8	326	48392	0.0431 ± 0.0190	[0.0399, 0.0463]	114.35
1/512	basic (3.8)	—	334	38879	0.0312 ± 0.0038	[0.0305, 0.0318]	440.91
	mollified (3.9)	3	352	40416	0.0332 ± 0.0049	[0.0324, 0.0340]	439.55
	mollified (3.9)	5	346	41128	0.0278 ± 0.0057	[0.0269, 0.0288]	352.47
	mollified (3.9)	8	374	47250	0.0195 ± 0.0072	[0.0183, 0.0207]	335.24

TABLE 4. Example 2: results for the basic scheme (3.8) and the mollified scheme (3.9) for different values of Δx and η .

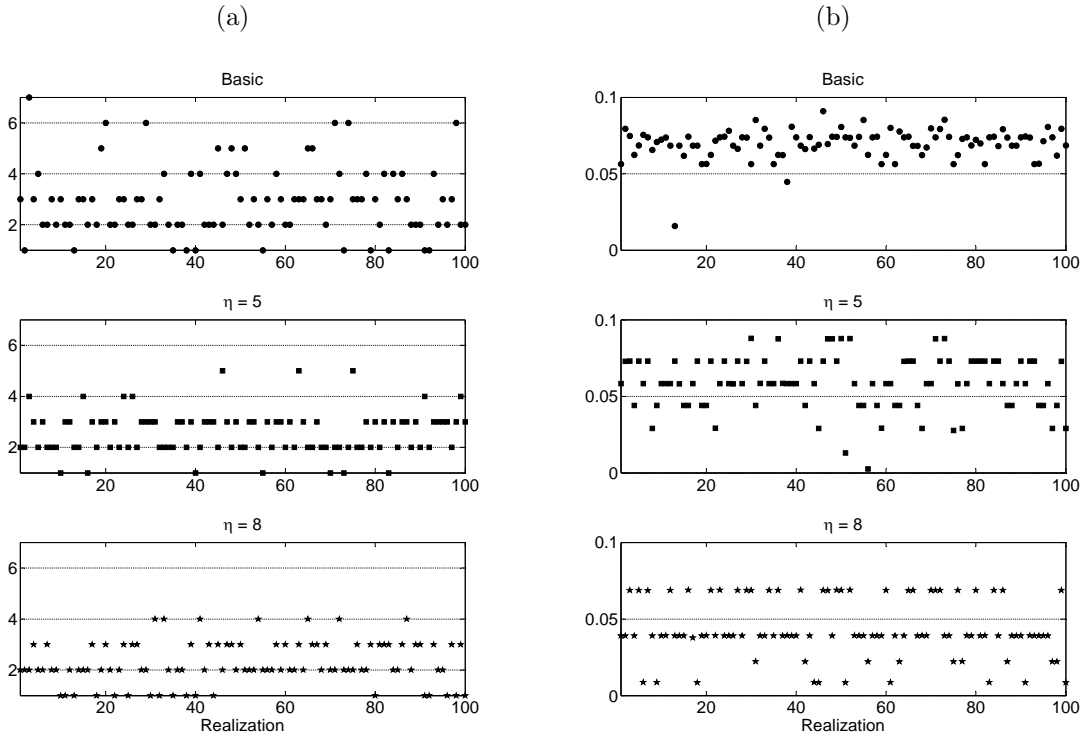


FIGURE 3. Example 2: (a) iterations of the restarted optimization algorithm, (b) resulting final relative error, for each realization of $\varphi = (\varphi_0, \dots, \varphi_{N-1})$.

5.3. **Example 3: sedimentation model, effect of noisy observation data.** Now we study the effect of working with noisy observation data. We randomly generate 100 final profiles and associate them to the

$\Delta x/L$	Scheme	η	# restarts	E_J	$\bar{e}_\infty \pm \sigma$	\mathcal{I}_∞	CPU [min]
1/128	basic (3.8)	—	359	50263	0.1360 ± 0.0476	[0.1280, 0.1439]	46.67
	mollified (3.9)	3	348	51086	0.1269 ± 0.0469	[0.1190, 0.1347]	55.57
	mollified (3.9)	5	327	47515	0.0936 ± 0.0428	[0.0864, 0.1007]	48.04
	mollified (3.9)	8	253	38949	0.0745 ± 0.0474	[0.0666, 0.0825]	37.13
1/256	basic (3.8)	—	385	50310	0.0661 ± 0.0264	[0.0617, 0.0705]	140.63
	mollified (3.9)	3	367	50489	0.0674 ± 0.0238	[0.0634, 0.0713]	152.60
	mollified (3.9)	5	368	52214	0.0533 ± 0.0256	[0.0490, 0.0575]	135.85
	mollified (3.9)	8	331	47153	0.0401 ± 0.0260	[0.0358, 0.0445]	110.56
1/512	basic (3.8)	—	346	39464	0.0308 ± 0.0163	[0.0281, 0.0335]	452.16
	mollified (3.9)	3	340	39954	0.0334 ± 0.0166	[0.0307, 0.0362]	436.76
	mollified (3.9)	5	366	43215	0.0274 ± 0.0150	[0.0249, 0.0299]	367.66
	mollified (3.9)	8	384	48706	0.0217 ± 0.0141	[0.0193, 0.0240]	346.08

TABLE 5. Example 3 with $\varepsilon = 0.01$: results for the basic scheme (3.8) and the mollified scheme (3.9) for different values of Δx and η .

ε	Scheme	η	# restarts	E_J	$\bar{e}_\infty \pm \sigma$	\mathcal{I}_∞	CPU [min]
0	basic (3.8)	—	388	48842	0.0696 ± 0.0096	[0.0680, 0.0712]	136.03
	mollified (3.9)	3	398	53513	0.0739 ± 0.0081	[0.0725, 0.0752]	160.74
	mollified (3.9)	5	355	48280	0.0587 ± 0.0174	[0.0558, 0.0616]	125.46
	mollified (3.9)	8	326	48392	0.0431 ± 0.0190	[0.0399, 0.0463]	114.35
0.01	basic (3.8)	—	385	50310	0.0661 ± 0.0264	[0.0617, 0.0705]	140.63
	mollified (3.9)	3	367	50489	0.0674 ± 0.0238	[0.0634, 0.0713]	152.60
	mollified (3.9)	5	368	52214	0.0533 ± 0.0256	[0.0490, 0.0575]	135.85
	mollified (3.9)	8	331	47153	0.0401 ± 0.0260	[0.0358, 0.0445]	110.56
0.03	basic (3.8)	—	376	49025	0.0801 ± 0.0554	[0.0709, 0.0894]	137.65
	mollified (3.9)	3	364	48447	0.0807 ± 0.0533	[0.0718, 0.0896]	146.72
	mollified (3.9)	5	374	50622	0.0760 ± 0.0528	[0.0672, 0.0848]	132.10
	mollified (3.9)	8	353	49136	0.0710 ± 0.0524	[0.0622, 0.0797]	115.31
0.05	basic (3.8)	—	378	49716	0.1163 ± 0.0913	[0.1011, 0.1316]	140.31
	mollified (3.9)	3	376	51246	0.1149 ± 0.0897	[0.0999, 0.1298]	156.50
	mollified (3.9)	5	359	50344	0.1129 ± 0.0902	[0.0979, 0.1280]	131.10
	mollified (3.9)	8	332	49139	0.1084 ± 0.0915	[0.0931, 0.1237]	115.54

TABLE 6. Example 3 with $\Delta x = L/256$: results for the basic scheme (3.8) and the mollified scheme (3.9) for different values of ε and η .

previously generated initial guesses. The corrupted profile is generated as follows:

$$u_j^\varepsilon = (1 + \varepsilon\varphi_j) u^{\text{obs}}(x_j), \quad j = 0, \dots, \mathcal{N} - 1,$$

where $\varepsilon = 0.01, 0.03$ and 0.05 , and φ_j is a uniformly distributed random variable assuming values between -1 and 1 . The results are presented in Tables 5 and 6 and Figure 4.

5.4. Example 4: traffic model, effect of a time-dependent observation. We consider a traffic “platoon” with density of 50 cars/mi, entering an initially empty road segment of length $L = 3.5$ mi at $x = 0$. At arriving to de point $x = 1$ a traffic light changes to red. From that instant, we assume the traffic obeys (1.1) with a flux function f and the diffusion function a of the respective forms (3.5) and (3.7). The parameter values used are the same as those used in [3] and references cited therein, namely $C = e/7$, $\tau = 2$ s, $L_{\min} = 0.05$ mi, $u_{\max} = 200$ cars/mi and $\alpha = 0.1g$, where $g = 9.81$ m/s² is the acceleration of gravity. The

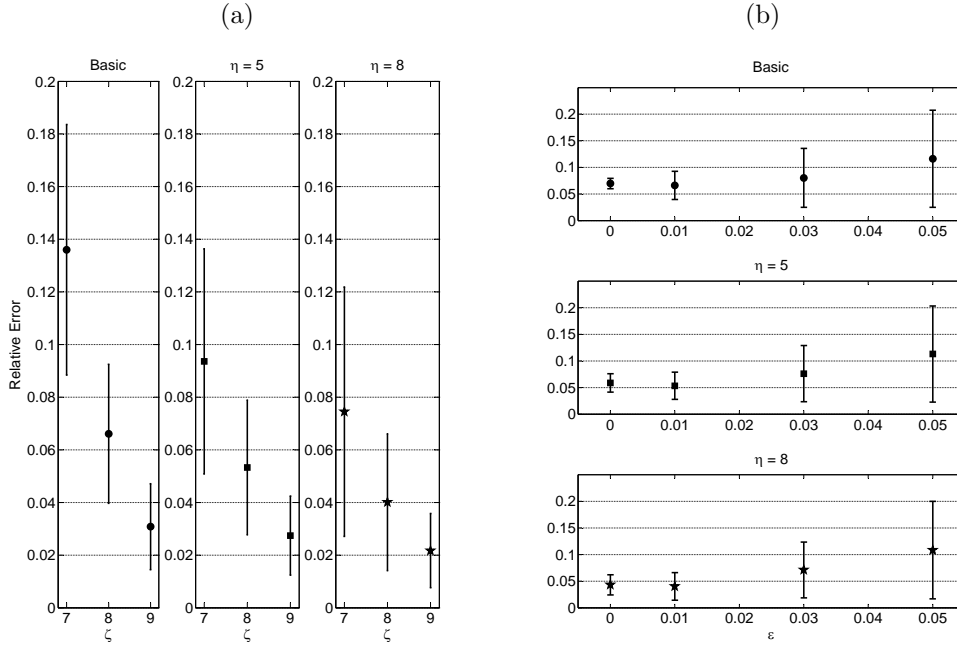


FIGURE 4. Example 3: (a) mean \bar{e}_∞ and standard deviation σ of the relative error versus spatial resolution $\zeta = \log_2(1/\Delta x)$ for $\epsilon = 0.03$, (b) mean \bar{e}_∞ and standard deviation σ of the relative error versus level of noise in the final profile at $\Delta x = 1/256$.

targets for our identification procedure are C and τ . Again the parameters for the optimization are $M = 10$ and $\epsilon = 10^{-4}$.

The traffic light changes from red to green and vice-versa every 30 seconds. When the light shows “red”, we will consider the road divided into the segments $[0, 1]$ and $[1, 3.5]$. The traffic light works as an impermeable boundary condition between these two regions. At the point $x = 0$ we assume that the platoon continues entering with the same density. Beyond the point $x = 3.5$ we suppose the road continues empty. When the light changes to green we work with the whole domain $[0, 3.5]$. Finally, for computing $JA(u^n)$ with red light, on $[0, 1]$ we extend the density beyond 1.0 by the constant u_{\max} , so the drivers cannot advance. On the domain $[1, 3.5]$ we extend the density by zero to the left of $x = 1.0$ because the drivers will feel nobody is coming from there. All these assumptions rely on the framework of (1.1) with $\psi_0 = 0$ and $\psi_L = 0$.

For the experiments the temporal observation is done at $x = 1.25$ from 0 to 2 seconds, starting with the red light. The selected spatial resolution was $\Delta x = 1/128$ and by A, B, C and D we denote the choices of the initial parameters $(0.7u_c, 0.7\tau)$, $(0.7u_c, 1.3\tau)$, $(1.3u_c, 0.7\tau)$ and $(1.3u_c, 1.3\tau)$, respectively. The results are summarized in Table 7, following the notation in Example 1.

5.5. Conclusions. Concerning Example 1, we observe that according to Table 3, the identifications based on the basic scheme and the mollified scheme produce good approximations of the parameter values. However, clearly the best performance is obtained by the mollified scheme with $\eta = 8$, not only with respect to CPU time, but also in terms of the regularity of approximation found and the error level. The behaviour with $\eta = 3$ is also very consistent. For the basic scheme and the mollified scheme for $\eta = 5$ we obtain more variability. In fact, for the initial guess A the method for $\eta = 5$ does not converge, but it does converge when started with initial guesses close to A.

The results in Table 4, corresponding to Example 2, illustrate how by improving the spatial resolution (i.e., reducing Δx) the quality of the identification result is increased. Note that, for each method, when

IG	j	\mathbf{p}_j	E_J	e_∞	CPU [s]	j	\mathbf{p}_j	E_J	e_∞	CPU [s]
Basic scheme					Mollified scheme with $\eta = 3$					
A	2	(0.3883,0.0006)	87	2.2682e-3	1063	2	(0.3883,0.0006)	84	3.9249e-3	920
B	3	(0.3883,0.0006)	100	1.9572e-3	1101	3	(0.3883,0.0006)	100	1.9572e-3	1110
C	2	(0.3883,0.0006)	91	1.7986e-3	894	2	(0.3883,0.0006)	87	9.1335e-4	947
D	2	(0.3883,0.0006)	94	4.7792e-3	884	2	(0.3883,0.0006)	93	4.7792e-3	790
Mollified scheme with $\eta = 5$					Mollified scheme with $\eta = 8$					
A	2	(0.3883,0.0006)	84	3.9249e-3	581	2	(0.3884,0.0006)	89	9.2882e-4	294
B	2	(0.3883,0.0006)	75	4.3762e-3	577	2	(0.3883,0.0006)	83	1.5402e-3	330
C	3	(0.3884,0.0006)	114	2.8443e-3	705	2	(0.3883,0.0006)	70	3.2157e-3	229
D	2	(0.3883,0.0006)	92	4.7792e-3	601	2	(0.3883,0.0006)	79	2.0756e-3	292

TABLE 7. Example 4: results for the basic scheme (3.8) and the mollified scheme (3.9) with $\eta = 3, 5$ and 8 .

Δx is decreased, the resulting values of the average \bar{e}_∞ of e_∞ and its standard deviation σ are also reduced. Again, the best results are for $\eta = 8$, this is evident in Figure 3 where its requirements of restarting and final errors are not only smaller but also more regular (less sensitive to the initial guess).

On the other hand, Example 3 illustrates the robustness of the proposed parameter identification procedure with respect to the presence of noise in the data. Table 5 shows how for a fixed level of noise by improving the spatial resolution the quality of the results improve. Figure 4 clearly indicates that the level of noise influences the quality of the recovery, but that in no case stability is lost.

Example 4 illustrates the applicability of the proposed identification procedure to an alternative strongly degenerate problem of great interest. The results endorse our previous remarks. But now, all the mollified versions produce better results than the basic version, not only in CPU time but also in the quality of the identification (error level).

Summarizing, we can say that the parameter identification procedure yields good results for both the basic scheme and its mollified versions. In particular, the mollification device leads to numerical results that are consistent between the spatial resolution, the noise level, the width of the mollification stencil and the quality of the identification results. Moreover, the mollified approach returned advantages not only in CPU time, but also in the error level and the sensitivity to the initial guess and to the noise in the data.

ACKNOWLEDGEMENTS

RB acknowledges support by Fondecyt project 1090456 and project BASAL CMM/Universidad de Chile and Centro de Investigación en Ingeniería Matemática (CI²MA), Universidad de Concepción.

CDA and CEM acknowledge support by COLCIENCIAS project 1118-48925120 and by grants from Vicerrectoría de Investigación, Universidad Nacional de Colombia.

REFERENCES

- [1] R. Bürger, K.H. Karlsen, On some upwind schemes for the phenomenological sedimentation-consolidation model, *J. Eng. Math.* 41 (2001) 145–166.
- [2] S. Berres, R. Bürger, K.H. Karlsen, E.M. Tory, Strongly degenerate parabolic-hyperbolic systems modeling polydisperse sedimentation with compression, *SIAM J. Appl. Math.* 64 (2003) 41–80.
- [3] R. Bürger, K.H. Karlsen, On a diffusively corrected kinematic-wave traffic model with changing road surface conditions, *Math. Models Methods Appl. Sci* 13 (2003) 1767–1799.
- [4] E. Rouvre, G. Gagneux, Solution forte entropique de lois scalaires hyperboliques-paraboliques dégénérées, *C. R. Acad. Sci. Paris Sér. I* 329 (1999) 599–602.
- [5] R. Bürger, S. Evje, K.H. Karlsen, On strongly degenerate convection-diffusion problems modeling sedimentation-consolidation processes, *J. Math. Anal. Appl.* 247 (2000) 517–556.
- [6] H. Holden, K.H. Karlsen, K.-A. Lie, N.H. Risebro, *Splitting Methods for Partial Differential Equations with Rough Solutions*. European Mathematical Society, Zurich, Switzerland, 2010.

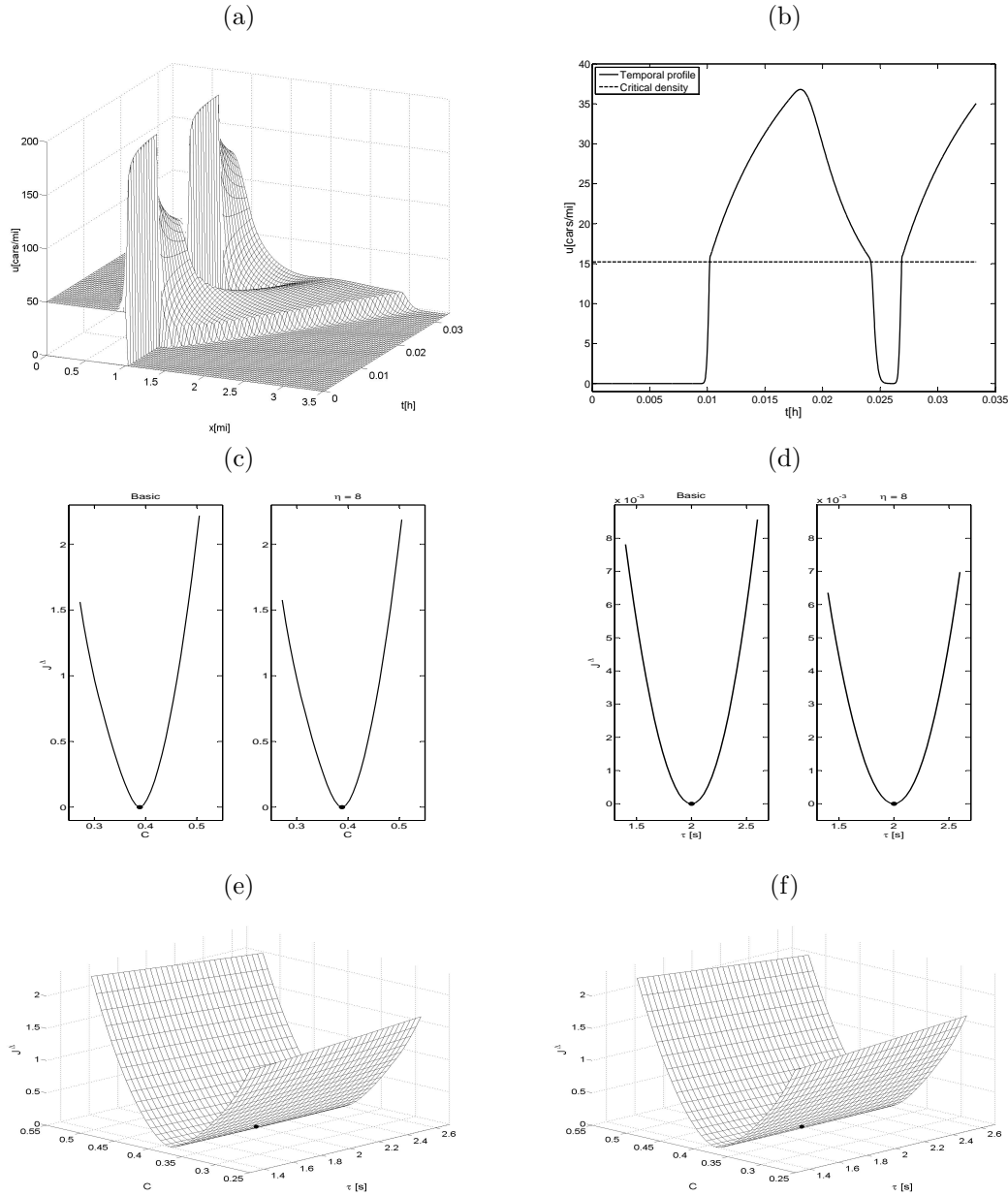


FIGURE 5. Example 4: (a) reference solution, (b) temporal profile u_{obs} for the definition of the cost functional; one parameter cost functional for (c) C and (d) τ ; two-parameter cost functional for the parameter set (C, τ) (e) for the basic scheme and (f) for the mollified scheme.

[7] S. Evje, K.H. Karlsen, Monotone difference approximations of BV solutions to degenerate convection-diffusion equations, *SIAM J. Numer. Anal.* 37 (2000) 1838–1860.
 [8] R. Bürger, A. Coronel, M. Sepúlveda, A semi-implicit monotone difference scheme for an initial- boundary value problem of a strongly degenerate parabolic equation modelling sedimentation-consolidation processes, *Math. Comp.* 75 (2006) 91–112.
 [9] C.D. Acosta, R. Bürger, C.E. Mejía, Monotone difference schemes stabilized by discrete mollification for strongly degenerate parabolic equations, *Numer. Meth. Partial Diff. Eqns.*, to appear.

- [10] C.E. Mejía, D.A. Murio, Numerical identification of diffusivity coefficient and initial condition by discrete mollification, *Comput. Math. Applic.* 30 (1995) 35–50.
- [11] C.E. Mejía, C.D. Acosta, K.I. Saleme, Numerical identification of a nonlinear diffusion coefficient by discrete mollification, submitted.
- [12] D.A. Murio, C.E. Mejía, Source terms identification for time fractional diffusion equation, *Rev. Colomb. Mat.* 42 (2008) 25–46.
- [13] R. Bürger, K.H. Karlsen, J.D. Towers, A mathematical model of continuous sedimentation of flocculated suspensions in clarifier-thickener units, *SIAM J. Appl. Math.* 65 (2005) 882–940.
- [14] R. Bürger, R. Ruiz-Baier, H. Torres, A stabilized finite volume element method for sedimentation-consolidation processes. Preprint 2011-15, Departamento de Ingeniería Matemática, Universidad de Concepción; submitted.
- [15] A. Coronel, F. James, M. Sepúlveda, Numerical identification of parameters for a model of sedimentation processes, *Inverse Problems* 19 (2003) 951–972.
- [16] S. Berres, R. Bürger, A. Coronel, M. Sepúlveda, Numerical identification of parameters for a strongly degenerate convection-diffusion problem modelling centrifugation of flocculated suspensions, *Appl. Numer. Math.* 52 (2005) 311–337.
- [17] S. Berres, R. Bürger, R. Garcés, Centrifugal settling of flocculated suspensions: a sensitivity analysis of parametric model functions, *Drying Technol.* 28 (2010) 858–870.
- [18] R. Bürger, A. Coronel, M. Sepúlveda, Numerical solution of an inverse problem for a scalar conservation law modelling sedimentation. In: E. Tadmor, J.-G. Liu and A.E. Tzavaras (eds.), *Hyperbolic Problems: Theory, Numerics and Applications. Proceedings of Symposia in Applied Mathematics*, vol. 67, Part 2. American Mathematical Society, Providence, RI, USA, 445–454 (2009).
- [19] D.A. Murio, *The Mollification Method and the Numerical Solution of Ill-Posed Problems*, John Wiley, New York, 1993.
- [20] D.A. Murio, Mollification and space marching, in: K. Woodbury (Ed.), *Inverse Engineering Handbook*, CRC Press, Boca Raton, 2002.
- [21] C.E. Mejía, D.A. Murio, Numerical solution of generalized IHCP by discrete mollification, *Comput. Math. Applic.* 32 (1996) 33–50.
- [22] C.D. Acosta, R. Bürger, Difference schemes stabilized by discrete mollification for degenerate parabolic equations in two space dimensions. Preprint 2011-04, Departamento de Ingeniería Matemática, Universidad de Concepción; submitted.
- [23] C.D. Acosta, C.E. Mejía, Stabilization of explicit methods for convection-diffusion problems by discrete mollification, *Comput. Math. Applic.* 55 (2008) 363–380.
- [24] M.C. Bustos, F. Concha, R. Bürger, E.M. Tory, *Sedimentation and Thickening*, Kluwer Academic Publishers, Dordrecht, 1999.
- [25] A.C. Dick, Speed/flow relationships within an urban area. *Traffic Engrg. Control* 8 (1996) 393–396.
- [26] H. Greenberg, An analysis of traffic flow. *Oper. Res.* 7 (1979) 79–85.
- [27] P. Nelson, Traveling-wave solutions of the diffusively corrected kinematic-wave model, *Math. Comp. Modelling* 35 (2002) 561–579.
- [28] P. Nelson, Synchronized traffic flow from a modified Lighthill-Whitham model, *Phys. Rev. E* 61 (2000) R6052–R6055.
- [29] B. Engquist, S. Osher, One-sided difference approximations for nonlinear conservation laws, *Math. Comp.* 36 (1981) 321–351.
- [30] C.D. Acosta and C.E. Mejía, Approximate solution of hyperbolic conservation laws by discrete mollification, *Appl Numer Math* 59 (2009), 2256–2265.
- [31] C.D. Acosta and C.E. Mejía, A mollification-based operator splitting method for convection-diffusion equations, *Comput Math Applic*, 59 (2010) 1397-1408.
- [32] J.C. Lagarias, J.A. Reeds, M.H. Wright, P.E. Wright, Convergence properties of the Nelder-Mead simplex method in low dimensions, *SIAM J. Optim.* 9 (1998) 112–147.
- [33] C.T. Kelley, Detection and remediation of stagnation in the Nelder-Mead algorithm using a sufficient decrease condition, *SIAM J. Optim.* 10 (1999) 43–55.
- [34] M.A. Luersen, R. Le Riche, Globalized Nelder–Mead method for engineering optimization, *Computers and Structures* 82 (2004) 2251–2260.
- [35] Q.H. Zhao, D. Urošević, N. Mladenovic, P. Hansen, A restarted and modified simplex search for unconstrained optimization, *Computers & Operations Research* 36 (2009) 3263–3271.
- [36] C.J. Price, I.D. Coope, D. Byatt, A convergent variant of the Nelder-Mead algorithm, *J. Optim. Theor. Appl.* 113 (2002) 5–19.

Centro de Investigación en Ingeniería Matemática (CI²MA)

PRE-PUBLICACIONES 2011

- 2011-07 EDWIN BEHRENS, JOHNNY GUZMAN: *A new family of mixed methods for the Reissner-Mindlin plate model based on a system of first-order equations*
- 2011-08 ALFREDO BERMÚDEZ, RAFAEL MUÑOZ-SOLA, CARLOS REALES, RODOLFO RODRÍGUEZ, PILAR SALGADO: *Mathematical and numerical analysis of a transient eddy current problem arising from electromagnetic forming*
- 2011-09 FABIÁN FLORES-BAZÁN, ELVIRA HERNÁNDEZ: *A unified vector optimization problem: complete scalarizations and applications*
- 2011-10 FABIÁN FLORES-BAZÁN, FERNANDO FLORES-BAZÁN, CRISTIAN VERA: *Gordan-type alternative theorems and vector optimization revisited*
- 2011-11 RODOLFO ARAYA, GABRIEL R. BARRENECHEA, ABNER POZA, FREDERIC VALENTIN: *Convergence analysis of a residual local projection finite element method for the Navier-Stokes equations*
- 2011-12 VERONICA ANAYA, MOSTAFA BENDAHMANE, MAURICIO SEPÚLVEDA: *Numerical analysis for HP food chain system with nonlocal and cross diffusion*
- 2011-13 FABIÁN FLORES-BAZÁN, ANTOINE SOUBEYRAN, DINH THE LUC: *Reference-dependent preferences and theory of change*
- 2011-14 RAIMUND BÜRGER, STEFAN DIEHL, SEBASTIAN FARÅS, INGMAR NOPEN: *Simulation of the secondary settling process with reliable numerical methods*
- 2011-15 RAIMUND BÜRGER, RICARDO RUIZ-BAIER, HECTOR TORRES: *A stabilized finite volume element method for sedimentation-consolidation processes*
- 2011-16 GABRIEL N. GATICA, ANTONIO MARQUEZ, SALIM MEDDAHI: *Analysis of the coupling of Lagrange and Arnold-Falk-Winther finite elements for a fluid-solid interaction problem in 3D*
- 2011-17 JESSIKA CAMAÑO, RODOLFO RODRÍGUEZ: *Analysis of a FEM-BEM model posed on the conducting domain for the time-dependent eddy current problem*
- 2011-18 CARLOS D. ACOSTA, RAIMUND BÜRGER, CARLOS E. MEJIA: *Numerical identification of parameters for strongly degenerate parabolic equations by discrete mollification*

Para obtener copias de las Pre-Publicaciones, escribir o llamar a: DIRECTOR, CENTRO DE INVESTIGACIÓN EN INGENIERÍA MATEMÁTICA, UNIVERSIDAD DE CONCEPCIÓN, CASILLA 160-C, CONCEPCIÓN, CHILE, TEL.: 41-2661324, o bien, visitar la página web del centro: <http://www.ci2ma.udec.cl>



**CENTRO DE INVESTIGACIÓN EN
INGENIERÍA MATEMÁTICA (CI²MA)
Universidad de Concepción**



Casilla 160-C, Concepción, Chile
Tel.: 56-41-2661324/2661554/2661316
<http://www.ci2ma.udec.cl>

